ISSN 0010-9525, Cosmic Research, 2016, Vol. 54, No. 1, pp. 67–75. © Pleiades Publishing, Ltd., 2016.

Electron Flux Variations at Altitudes of 600–800 km in the Second Half of 2014. Preliminary Results of an Experiment Using RELEC Equipment Onboard the Satellite *VERNOV*

I. N. Myagkova[a], M. I. Panasyuk[a, b], S. I. Svertilov[a, b], V. V. Bogomolov[a, b], A. V. Bogomolov[a], V. V. Kalegaev[a], V. O. Barinova[a], and E. A. Balan[a]

[a] *Institute of Nuclear Physics, Moscow State University, Moscow, Russia*

[b] *Faculty of Physics, Moscow State University, Moscow, Russia*

e-mail: irina@srd.sinp.msu.ru

Received April 2, 2015

Abstract—The results of measurements of fluxes and spectra carried out using the RELEC (relativistic electrons) equipment onboard the *VERNOV* satellite in the second half of 2014 are presented. The *VERNOV* satellite was launched on July 8, 2014 in a sun-synchronous orbit with an altitude from 640 to 830 km and an inclination of 98.4°. Scientific information from the satellite was first received on July 20, 2014. The comparative analysis of electron fluxes using data from RELEC and using experimental data on the electron detection by satellites *Elektro-L* (positioned at a geostationary orbit) and *Meteor-M no. 2* (positioned at a circular polar orbit at an altitude of about 800 km as the *VERNOV* satellite) will make it possible to study the spatial distribution pattern of energetic electrons in near-Earth space in more detail.

DOI: 10.1134/S0010952516010135

INTRODUCTION

Currently, the understanding of the variation mechanisms of fluxes and spectra of relativistic and subrelativistic electrons of the outer radiation belt of the Earth at altitudes up to 1000 km during geomagnetic disturbances of varying intensity, both extremely strong and weak disturbances, remains one of the most pressing problems of space weather. Almost from the discovery of the outer radiation belt of the Earth (ERB) it has been clear that it is influenced by competing processes of the acceleration and scattering of particles, and these processes are not linear. However, until the present time there has been no commonly accepted theory of electron acceleration to relativistic energies in the Earth's magnetosphere. Existing models of acceleration and scattering of particles, such as wave–particle interaction (e.g., [1–3]), local magnetic traps in the auroral oval [4], and radial diffusion [5, 6] do not describe the collection of available experimental data and do not make it possible to reliably predict variations of the outer ERB as a result of geomagnetic disturbances. Experimental data that in only about half of the cases does the electron flux in the outer ERB increase after a magnetic storm compared to the one before the storm [7], regardless whether it is caused by the coronal mass ejection (CME) approaching the Earth or a solar wind high-speed stream (SWHSS), have not yet found a theoretical explanation.

On the other hand, the monitoring of radiation conditions in near-Earth space (NES) is necessary for space flights, in particular, in order to prevent malfunctions of electronic equipment onboard spacecraft in the case of sharp rises in the fluxes of relativistic electrons of the ERB during the recovery phase of geomagnetic storms (e.g., [8, 9]).

Therefore, new experimental data on the dynamics of the outer ERB, which have high time resolution and make it possible to estimate the pitch-angle distribution of electrons, appear to be relevant. The study of variations fluxes and spectra of trapped and precipitating relativistic electrons in the NES was one of the main objectives of the experiment, using the scientific equipment RELEC onboard the *VERNOV* satellite (MKA-FKI (PN2)), along with gamma-ray bursts from the Earth's atmosphere and the study of the connection between atmospheric light transient phenomena with the precipitation of relativistic electrons from Earth's radiation belts.

This paper presents the preliminary results of the detection of variations in fluxes of relativistic and subrelativistic electronics by the RELEC equipment onboard the *VERNOV* satellite in July to December 2014 that show the potential of this experiment with respect to the study of outer ERB variations and bursts of the intensity of fluxes of electrons with the energy of a hundred keV at auroral and middle latitudes.

EXPERIMENTAL

The *VERNOV* satellite was launched into a sun-synchronous orbit (with an apogee of 830 km, a perigee of 640 km, an inclination of 98.4°, weight of 283 kg, and an orbital period of 100 min) on July 8, 2014.

In order to measure the fluxes and spectra of trapped and precipitating electrons, the instrument DRGE (detectors for study of X-rays, gamma-rays, and electrons) was used. This instrument can detect hard electromagnetic radiation (energy range 0.01–3.0 MeV), relativistic and subrelativistic electrons (energy range 0.2–15 MeV), and protons with energies of 5–100 MeV. The instrument consists of three modules: two identical modules DRGE-1 and DRGE-2 and module DRGE-3, consisting of three identical detectors. In this paper, we used data from the module DRGE-3.

Each of the phoswich detectors of DRGE-3 is made of crystals CsI(Tl) (0.3 cm thickness, 2.0 cm diameter) and BGO (1.7 cm thickness, 2.0 cm diameter) sampled by a photomultiplier. The assembly CsI(Tl)/BGO with a collimator, which is a cylinder with a height of 1.0 cm, the diameter of 2 cm, and a wall thickness of 0.1 cm, is placed into a glass made of a plastic scintillator based on polystyrene with a thickness of 0.5 cm, which makes it possible to avoid the detection of charged particles reaching the detector outside its field of view. Signals from different scintillators are separated by electronic methods based on the different durations of the current pulse at the output of the PMT because of different scintillation decay times. Therefore, scintillators with significantly different decay times are used as components of the phoswich detector. Events related to the detection of electrons and X-rays can be separated by the ratio of energy release quantities in crystals CsI and BGO, using methods of amplitude analysis. In the range from 0.2 to 1.5 MeV, electrons are detected by the full absorption in CsI(Tl), and in the range from 1.5 to 15 MeV, by energy releases >1.5 MeV in the crystal BGO. Eight energy channels are selected for CsI and BGO: 200–235, 235–300, 300–400, 400–570, 570–850 keV, 0.85–1.35, 1.35–2.15, 2.15–3.15 MeV and 3.2–3.25, 3.25–3.45, 3.45–3.8, 3.8–4.4, 4.4–5.4, 5.4–7.5, 7.5–11, 11–18 MeV, respectively.

The axes of the three detectors of the module DRGE-3 in the standard spacecraft operation mode are directed as follows: the axis of detector no. 1 (DRGE-31) is directed to the local zenith, the axis of detector no. 2 (DRGE-32) is parallel to SC trajectory, against the SC velocity vector, and the axis of detector no. 3 (DRGE-33) is at an angle of 90° to the plane formed by the velocity vector and the direction to the local zenith. The orientation accuracy of axes of detectors is ±3°. This orientation of detectors means that to the first approximation, it can be assumed that DRGE-31 detected trapped particles at low latitudes and precipitating particles at high latitudes. DRGE-32, on the contrary, detected precipitating particles near the equator and trapped particles in the outer ERB. DRGE-33 detected trapped particles along the whole orbit. The detailed description of the operation principle and physical and technical characteristics of DRGE will be published in the future.

EXPERIMENTAL DATA

Figure 1 shows an example of the time dependences of count rates of three detectors of the module DRGE-3 in channels of 230–300 and 570–850 keV, which were recorded for two and a half hours on September 18, 2014, from 14.30 to 17.00 UT.

The bottom panel of Fig. 1 shows readings of DRGE-31 according to lower curves (the solid black curve indicates 230–300 keV and the gray curve corresponds to 570–850 keV), of DRGE-32, by the curves second from the bottom (the gray solid curve indicates 230–300 keV and the black curve corresponds to 570–850 keV), of DRGE-33, by the curves third from the bottom (the black dashed curve indicates 230–300 keV and the gray dashed curve corresponds to 570–850 keV), and at the top panel the number of the L-shell is given (the solid black curve indicates the McIlwain parameter and the gray dot-dash curve corresponds to magnetic local time (MLT)).

Time profiles of the fluxes of electrons with energies of 235–300 and 570–850 keV recorded by DRGE-3 and shown in Fig. 1 are typical for experiments on SC with a low polar orbit: an increase in the count rates is observed from the equator to higher latitudes, five intersections of the outer ERB can be seen (14.45, 15.00, 15.35, 15.48, and 16.22 UT). In periods between 14.45 and 15.00, as well as between 15.35 and 15.48, the satellite is at the polar cap. From Fig. 1, it can be seen that during the passage of the outer ERB, count rates of trapped electrons detected by DRGE-32 and DRGE-33 in the channel of 235–300 keV (gray and black dashed curves, respectively) are predictably higher than the count rates of precipitated electrons (indications from DRGE-31, the lower black solid curve). Regarding the channel of 570–850 keV, Fig. 1 shows that for DRGE-32 and DRGE-33 in the morning sector, with respect to the MLT, count rates in both channels are similar, while in the evening sector with respect to MLT, count rates in the channel of 570–850 keV are significantly lower. For DRGE-31, which measures particles precipitating from the outer ERB, count rates in channel of 570–850 keV are lower than at any MLT. That is, Fig. 1 shows that the spectrum of electrons of the outer ERB at low altitudes depends on the local time and possibly on the longitude of the measurement point.

Another feature of readings from three detectors DRGE3 is the presence of weak rises in the morning sector at the equator (see, 16.00–16.10), not only in the channel of 230–300 keV but also in the channel of

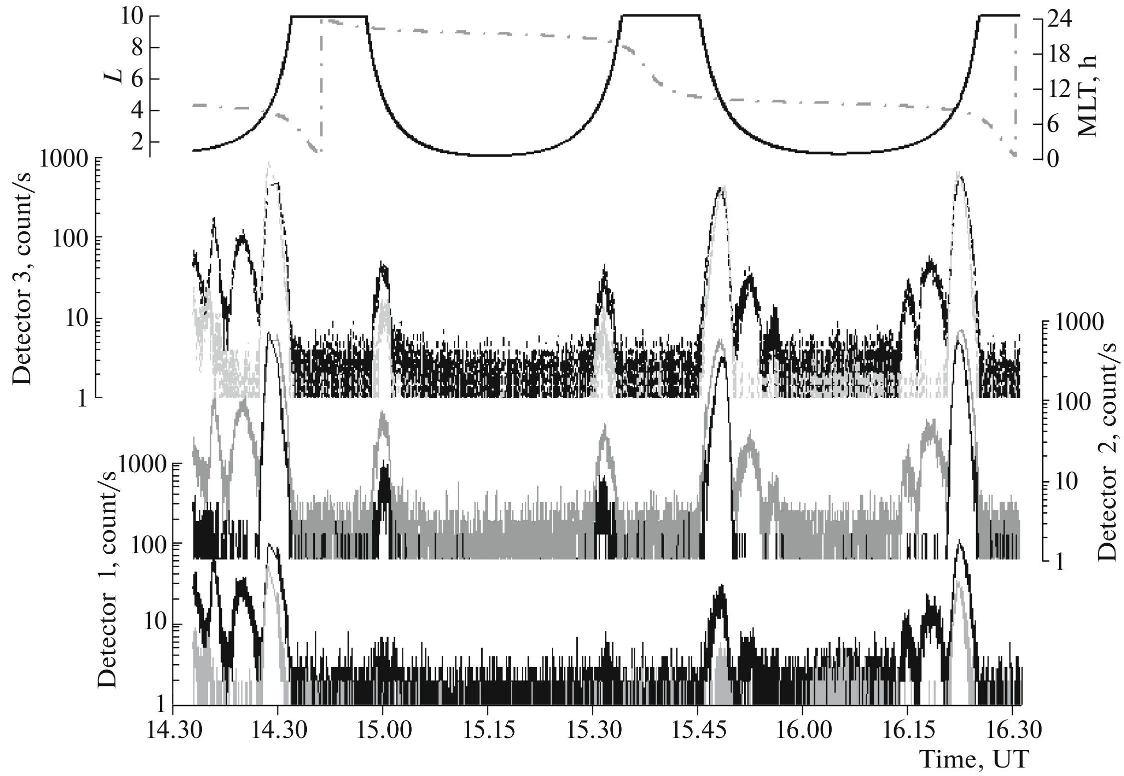

Fig. 1. Time dependences of count rates of the detector DRGE-3 RELEC.

570–850 keV, characteristic of DRGE-31 (a gray curve at the bottom panel), and to a lesser extent, of DRGE-33 (third bottom panel, a gray dotted line). For DRGE-32 there are no such equatorial rises; i.e., at the equator there is a slight rise in the flux of trapped electrons and no precipitating particles are observed.

In addition to passages of the outer ERB, intense rises of fluxes of electrons in the gap between radiation belts at 14.36 and 14.40 UT can be noted in Fig. 1, as well as rises in the interval between 15.50 and 16.20, the peaks of which correspond to L = 1.7 and 2.2. Rises of the fluxes of electrons with energies of a hundred keV on these L were detected earlier: for example, in experiments onboard satellites *OHZORA* [10] and *CORONAS-I* [11, 12], but with regard to the peak in the gap, it should be noted that the presence of two (instead of one) additional peaks of intensity is not typical for this area of near-Earth space. From Fig. 1 it is clear that what has been said regarding rises of the fluxes of electrons by L = 2.2 and 1.7–1.8 refers only to the 230–300 keV channel; such rises are not observed in the channel of 570–850 keV except for the detector DRGE-33, where a rise in the gap by L = 1.7 can be seen in 570–850 keV channel (gray dotted line in the third bottom panel, the maximum at 14.33 UT).

The count rate profiles of all three detectors DRGE-3 presented in Fig. 1, depending on L (McIlwain parameter), are given in Fig. 2a. Black curves show an interval of 14.35–14.50, where the *VERNOV* satellite passed near the center of the Brazilian magnetic anomaly (BMA) and gray curves, the interval of 16.10–16.25, i.e., during the next turn. The top panel shows the profile of fluxes of electrons with energies >100 keV, measured by the MSGI instrument onboard the *Meteor-M no. 2* satellite, which has an orbit of 825 km with an inclination of 98.8 degrees, which traversed the same regions of space as the *VERNOV* satellite some time later. From Fig. 2a it can be seen that the profiles according to data from RELEC *VERNOV* and *Meteor-M no. 2* match well. There are also two peaks in the gap between the belts in the data from *Meteor-M no. 2.*

Figure 2a shows that the peak position on L between 2 and 3 (maximum L = 2.2) is maintained while moving to a different longitude and changes the intensity very slightly. However, the peak at L = 1.7 at a distance from the BMA shifts to higher L (1.8) according to both experiments, and its intensity on the *VERNOV* orbit drops, while, according to *Meteor-M no. 2* it, on the contrary, increases. It is planned to conduct a detailed comparison of the bursts of electrons based on data from different experiments.

Figure 2b shows the profiles according to L similar to Fig. 2a for six channels of DRGE-33. Figure 2b shows that the polar border of the outer ERB is gradually shifting from L = 12 for 200–235 keV to L = 8 for 0.85–1.35 MeV and the maximum, on the contrary, moves to lower L, although, because of the lack of

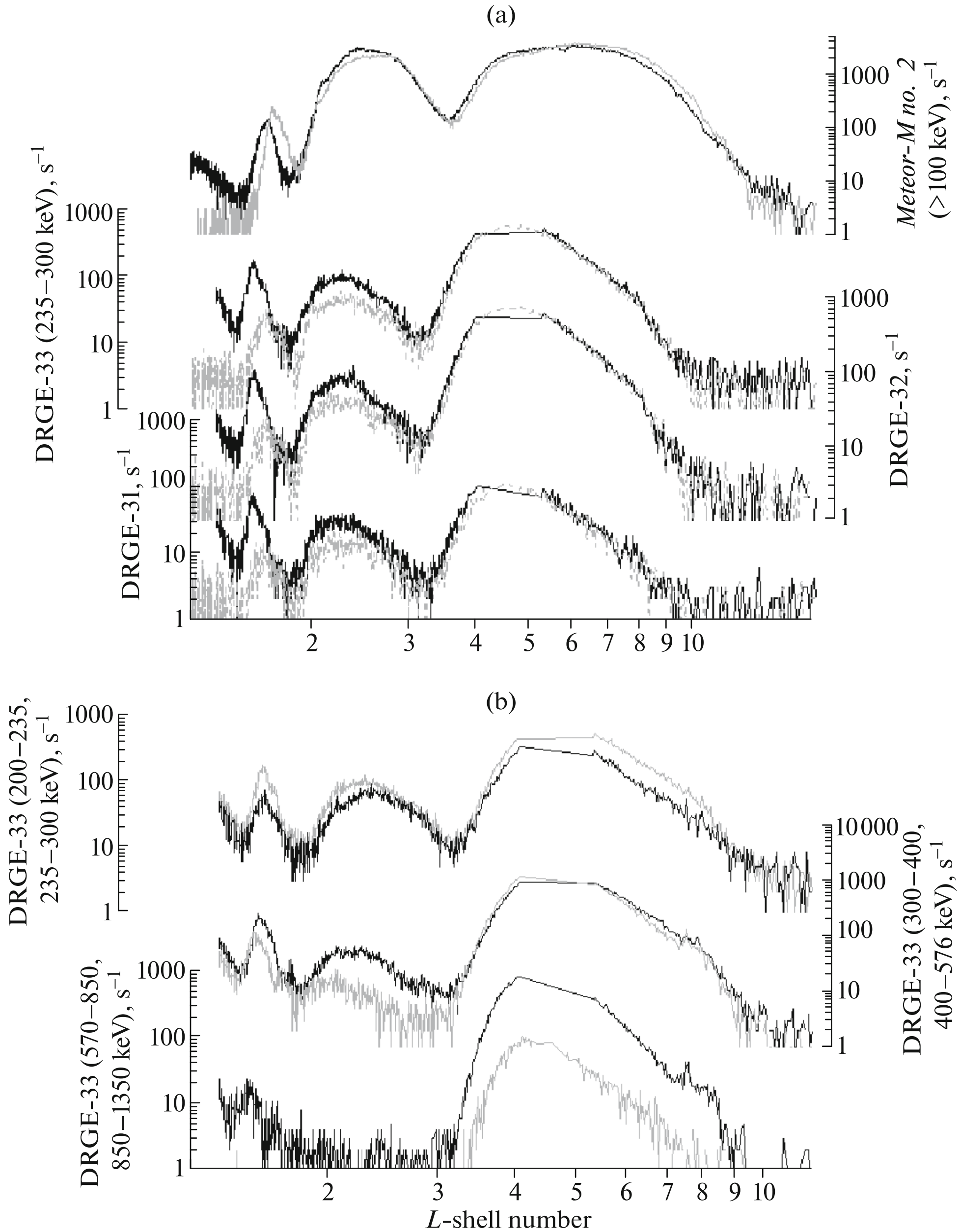

Fig. 2. Electron count rate profiles by the instrument DRGE-3 (RELEC) depending on L.

data, it is possible to confidently estimate the position of the maximum only starting from 850 keV. With regard to the energy limits of additional peaks in the gap, Fig. 2b shows that the peak at $L = 1.7$ is harder and vanishes only above 850 keV, and at $L = 2.2$ it is above 570 keV.

SPATIAL DISTRIBUTION OF FLUXES OF ELECTRONS ACCORDING TO DATA OF THE VERNOV SATELLITE

Figure 3 shows a map of the distribution of count rates of electrons with energies of 235–300 keV in geographic coordinates recorded by the detector no. 1 DRGE-3 of the RELEC equipment onboard the *VERNOV* satellite during September 2014. Open circles indicate the geographical position of turns shown in Fig. 1.

This map was obtained by the superimposition of DRGE-31 count rates along the projections of successive orbits. It gives an idea of the spatial distribution of intensity fluxes of electrons with energies of 235–300 keV at satellite altitudes of 600–800 km trapped near the equator and precipitating in the outer ERB. As mentioned above, empty circles on this map indi-

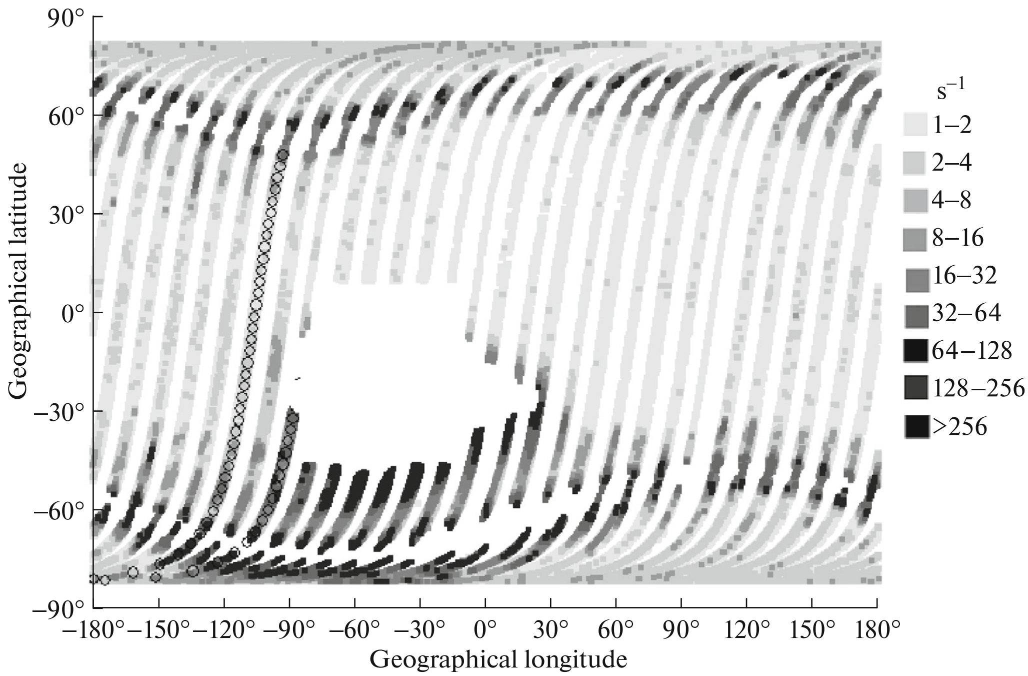

Fig. 3. Map of counting rates of electrons according to RELEC equipment on board the *VERNOV* satellite.

cate the geographical position of satellite passages shown in Fig. 1.

The map clearly shows the areas with increased electrons fluxes noted above: the outer radiation belt in the north and the south, the edge of the inner radiation belt (white areas indicate a lack of data), and rises of fluxes in mid-latitudes. In addition to rises in fluxes in the outer ERB on longitudes to the west of the BMA (longitude ranges from −180° to −90°), as well as at longitudes of 105° to 180°, there can be seen rises (bursts) of the intensity of the fluxes of electrons that are shown by darken areas on the map at mid-latitudes (L = 1.7–1.8, and L = 2.2–2.3). Qualitatively, this map coincides with a similar map of bursts of electrons with energies of hundreds of keV obtained in the experiment on the *CORONAS-I* satellite [11, 12].

VARIATIONS OF OUTER ERB ACCORDING TO DATA FROM RELEC ONBOARD THE *VERNOV* SATELLITE ON SEPTEMBER 2014

For four and a half months from July to December 2014 of the flight of the *VERNOV* satellite in the magnetosphere, there were only three moderate storms: at the end of August, in September, and in early November. Let us consider the September storm because of the variations in electron fluxes according to data from DRGE-3 of the RELEC equipment of the *VERNOV* satellite.

The geomagnetic storm that began on September 12, 2014 was caused by the arrival of two CMEs to the Earth. The first of them was accompanied by the class *M4.5* flare that occurred on September 9, 2014, in the active region (AR) 2158, and the second was associated with the flare X1.6, which occurred in the same AR on the next day, September 10, 2014. As a result, close to midnight from September 12 to September 13, 2014, solar wind speed exceeded 700 km/s (a black curve on the bottom panel of Fig. 4), but the z-component of the interplanetary magnetic field (the gray curve in the bottom panel of Fig. 4) turned to the south. It was negative only for a very short time, less than an hour. Thus, the maximum amplitude of the *Dst*-variation (the gray line in the central panel of Fig. 4) reached −75 nT, and the maximum value of the *Kp* index was 6.7 (the black line in the middle panel of Fig. 4). However, this storm caused noticeable flux variations in the outer ERB. Figure 4 shows time dependences of the counting rate of relativistic electrons in the channel with the energy of 1.35–2.15 MeV measured by detectors DRGE-31 (black triangles) and DRGE-32 (gray squares). Data from DRGE-3 were averaged for each satellite passage in a given range of values of L for the range of longitudes 60°–120° of the eastern longitude in the Northern Hemisphere. Count rates obtained at lower L, L = 3–4, are shown by open symbols, and L = 5–6 are depicted by closed ones. Values of the electron flux >2 MeV in the geostationary orbit according to data from the *GOES* satellite averaged over a day in order to avoid diurnal variation are shown in the top panel of Fig. 4.

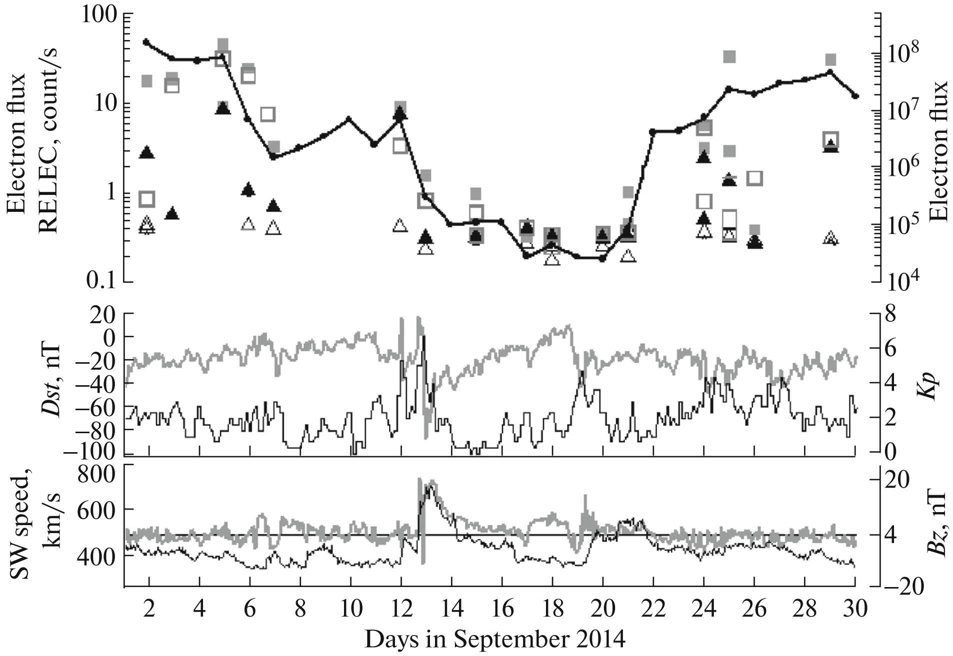

Fig. 4. Time dependences of count rate of relativistic electrons according to data from DRGE-3 RELEC of *VERNOV* and *GOES* satellites during geomagnetic storm of September 2014.

Figure 4 shows that according to data from the *GOES* satellite, the time variation of the fluxes of electrons with energies >2 MeV in the geostationary orbit agrees qualitatively with the data from DRGE-3, and, as might be expected, the best match is observed at higher L (closed symbols), since the geostationary orbit is $L = 6.6$, and for the data of DRGE-32 the match is better than for DRGE-31 because in the outer ERB, DRGE-32 records trapped particles and DRGE-31 records precipitating ones.

The significant spread of data from DRGE-3 is associated with the longitudinal dependence of electron fluxes typical for low-altitude polar orbits (e.g., [13]) observed even in a predetermined relatively narrow range of longitudes.

Figure 4 shows that variations of the fluxes of relativistic electrons on both the geostationary orbit and the *VERNOV* orbit do not fully comply with the typical scenario noted in many previous studies (e.g., [13–15], the decrease of electron fluxes of the outer ERB on the main phase and their subsequent increase). In this case, we see a significant difference from the usual scenario, i.e., a decrease of electron fluxes in the outer ERB on both the geostationary orbit and the *VERNOV* orbit continued not only on the main phase but also during the recovery phase. The increase of the electron flux of the outer ERB began after another, weaker geomagnetic disturbance on September 19, 2014. The physical cause of the disturbance on September 19, 2014 is the turn to the south of the z-component of the IMF accompanied by a sharp increase in the density of the solar wind (up to 40 particles per cubic centimeter) at a relatively low speed of the solar wind, only 500 km/s. The maximum of the *Dst*-variation amplitude was only −36 nT, *Kp* index was 4.7. Nevertheless, this was sufficient for an increase of electron fluxes of the outer ERB by more than an order of magnitude. Figure 4 also shows that, as in the earlier experiments, for example, on satellites of the *CORONAS* series [14, 16], electron fluxes of the outer ERB recover faster after a storm at high L compared to small values, but still somewhat later than on the geostationary orbit. In the future, it is planned to carry out a more detailed study of the causes of this dynamic of the outer ERB according to data not only from the RELEC equipment but also from other domestic and foreign SC.

INCREASE OF ELECTRON FLUXES ON THE POLAR BOUNDARY OF THE OUTER RADIATION BELT

Figure 5 shows the count rate profiles of three detectors of DRGE-3 depending on the McIlwain parameter L obtained approximately at 13.00 on October 12, 2014, in the night sector (about 22.00 MLT) for channels of 230–300 keV (DRGE-31 is the grey dotted line and black dots, DRGE-32 is the gray open points, and DRGE-33 is the solid black line and straight black crosses) and 570–850 keV (DRGE-31 is the black dotted line and oblique crosses, DRGE-32 is the gray solid line, and DRGE-33 is the black solid line). Figure 5 clearly shows that in the maximum of

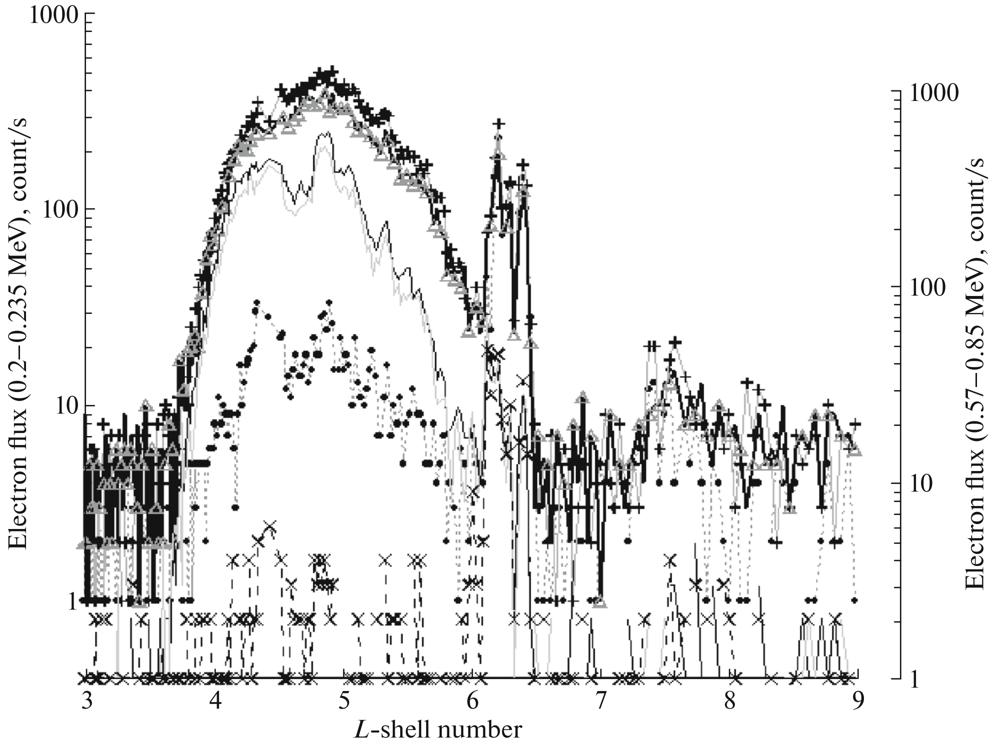

Fig. 5. Profiles of counting rates of detectors DRGE-3 RELEC depending on L.

the outer ERB that falls on $L = 4.5–4.7$, count rates of DRGE-33 and DRGE-32, which detect trapped particles, are almost the same for both energy channels, and the count rate of DRGE-31, which detects trapped particles, is about an order of magnitude smaller than for 230–300 keV and one and half order for 570–850 keV. However, at the polar boundary of the outer ERB, in the region of $L = 6–6.5$, count rates of all three detectors in both energy channels are the same; i.e., an isotropization of fluxes occurs at the boundary of the outer ERB.

Such structures are regularly observed by low-altitude polar satellites, such as *NOAA POES* or *Meteor-M no. 1.* They are well studied, and their characteristics have been used successfully to determine the state of the magnetosphere [17–19]. The circumpolar edge of the region of adiabatic motion of particles in the outer radiation belt is adjacent to the region of intense electron precipitations, the so-called *energetic electron arc* (EEA). These phenomena are associated with electron scattering, because of the small radius of curvature at subequatorial regions of field lines. They can be seen in quiet and disturbed geomagnetic conditions [19]. In [17], based on simultaneous measurements of the satellites *NOAA POES*, *Themis*, and *DMSP*, it was shown that in their most pronounced form, EEAs are observed in the preliminary phase of a substorm or on the eve of breakup, a sudden onset of a substorm. The period of 12.00–18.00 UT on October 12, 2014, was characterized by a moderate substorm disturbance, which may explain the intense electron precipitations in the circumpolar region of the outer radiation belt observed by the RELEC equipment.

This case is not unique. If we look at the map of the count rates of precipitating electrons shown in Fig. 3, we can see that darkened regions can be observed at the polar boundary of the outer ERB. We interpret them as flux isotropization regions similar to those described above. We assume that they are associated with substorm activity.

In addition to the burst by $L = 6–6.5$, Fig. 5 also shows a less intense but also isotropic increase of the counting rate of all the three detectors in the 235–300 keV energy channel with a maximum of $L = 7.5$, presumably in the auroral oval. We believe that this increase in the flux of energetic electrons in the auroral oval is similar to those described in [4, 20].

RESULTS AND DISCUSSION

On the one hand, data obtained using the equipment RELEC (DRGE-3) in the experiment on the *VERNOV* satellite do not contradict the results of earlier experiments. On the other hand, it makes it possible to specify the results, because of the detailed spectral and temporal resolution and because of the possibility to estimate the pitch angular distribution of the electron fluxes. Thanks to the simultaneous operation of the satellites *VERNOV* and *Meteor-M no. 2*, synchronous observations were conducted. It was found that the profiles of electron fluxes measured in these experiments agreed qualitatively.

Maps of electron flux rates according to data from DRGE-3 (Fig. 3) are consistent with maps of bursts of electrons with energies of hundreds of keV obtained in the experiment on the *CORONAS-I* satellite [11, 12]. The behavior of electron fluxes in the outer ERB, according to data from RELEC (DRGE-3), is similar to the nature of variations obtained by the authors of this paper in experiments on satellites of the *CORONAS* series [13–16]. The presence of three detectors with different directions made it possible to reveal moments of the isotropization of electron fluxes in the polar boundary of the outer ERB and to experimentally confirm that bursts of electrons in the auroral oval have an isotropic angular distribution.

CONCLUSIONS

Data presented in this paper showed that RELEC equipment, in particular the DRGE-3 instrument, mounted onboard the *VERNOV* satellite not only make it possible to measure fluxes and spectra of electrons in a wide range of energies, from 200 keV to 15 MeV, but also make it possible to estimate the pitch-angle distribution of particles. Thus, it is possible to experimentally investigate the connection between intensity variations, spectra of electrons of the Earth's outer radiation belt, and precipitating particles at different latitudes with geomagnetic disturbances, which will make it possible to better understand the mechanisms of the acceleration, propagation, and scattering of electrons in the Earth's magnetosphere.

An experiment using the RELEC (DRGE-3) equipment onboard the *VERNOV* satellite in July–December 2014 made it possible to discover the double rises of the fluxes of electrons with energies of hundreds of keV in the gap between ERBs. The reliability of this result is confirmed by the fact that in addition to the results of the *VERNOV* satellite, a similar profile was detected on the satellite *Meteor-M no. 2*. Data for the study of the anomalous behavior of electrons of the outer ERB during the September 2014 storm were obtained. Moments of isotropization of electron fluxes on the polar boundary of the outer ERB were revealed.

ACKNOWLEDGMENTS

This work was supported by the Russian Foundation for Basic Research, project no. RF MEF I60414X0049.

REFERENCES

1. Shprits, Y.Y., Meredith, N.P., and Thorne, R.M., Parameterization of radiation belt electron loss timescales due to interactions with chorus waves, *Geophys. Res. Lett.*, 2007, vol. 34, L11110. doi 10.1029/2006GL029050
2. Shprits, Y.Y., Subbotin, D., Ni, B., et al., Profound change of the near-Earth radiation environment caused by solar superstorms, *Space Weather*, 2011, vol. 9, no. 8. doi 10.1029/2011SW000662
3. Turner, D.L., Shprits, Y.Y., Hartinger, M., et al., Explaining sudden losses of outer radiation belt electrons during geomagnetic storms, *Nature Phys.*, 2012, vol. 8, pp. 208–212. doi 10.1038/nphys2185
4. Antonova, E.E., Myagkova, I.N., Stepanova, M.V., et al., Local particle traps in the high latitude magnetosphere and the acceleration of relativistic electrons, *J. Atmos. Sol.–Terr. Phys.*, 2011, vol. 73, nos. 11–12, pp. 1465–1471. doi 10.1016/j.jastp.2010.11.020
5. Brautigam, D.H. and Albert, J.M., Radial diffusion analysis of outer radiation belt electrons during the 9 October, 1990, magnetic storm, *J. Geophys. Res.*, 2000, vol. 105, no. A1, pp. 291–309. doi 10.1029/1999JA900344
6. Selesnick, R.S. and Blake, J.B., On the source location of radiation belt relativistic electrons, *J. Geophys. Res.*, 2000, vol. 105, no. A2, pp. 2607–2624. doi 10.1029/1999JA900445
7. Reeves, G.D., McAdams, K.L., Friedel, R.H.W., et al., Acceleration and loss of relativistic electrons during geomagnetic storms, *Geophys. Res. Lett.*, 2003, vol. 30, p. 1529. doi 10.1029/2002GL016513
8. Iucci, N., Leviti, A.E., Belov, A.V., et al., Space weather conditions and spacecraft anomalies in different orbits, *Space Weather*, 2005, vol. 3, no. 1, p. S01001. doi 10.1029/2003SW000056
9. Romanova, N. and Pilipenko, V., ULF wave indices to characterize the solar wind–magnetosophere interaction and relativistic electron dynamics, *Acta Geophys.*, 2008, vol. 57, no. 1, pp. 158–170.
10. Nagata, K., Kohno, T., Murakami, H., et al., Electron (0.19–3.2 MeV) and proton (0.58–35 MeV) precipitations observed by OHZORA satellite at low zones L = 1.6–1.8, *Planet. Space Sci.*, 1988, vol. 36, pp. 591–606.
11. Bashkirov, V.F., Denisov, Y.I., Gotselyuk, Y.V., et al., Trapped and quasi-trapped radiation observed by CORONAS-I satellite, *Radiat. Meas.*, 1999, vol. 30, no. 5, pp. 537–546.
12. Kuznetsov, S.N. and Myagkova, I.N., Quasi-trapped electron fluxes (>0.5 MeV) under the radiation belts: Analysis of their connection with geomagnetic indices, *J. Atmos. Sol–Terr. Phys.*, 2002, vol. 64, nos. 5–6, pp. 601–605.
13. Kuznetsov, S.N., Myagkova, I.N., Yushkov, B.Yu., et al., Dynamics of the Earth's radiation belts during strong magnetic storms according to KORONAS-F satellite data, *Astron. Vestn., Issled. Sol. Sist.*, 2007, vol. 41, no. 4, pp. 350–359.
14. Kuznetsov, S.N., Yushkov, B.Yu., Kudela, K., et al., Dynamics of the Earth's radiation belts during the magnetic storm of November 6th, *Adv. Space Res.*, 2005, vol. 36, no. 10, pp. 1997–2002.
15. Kuznetsov, S.N. and Myagkova, I.N., Energetic trapped proton and electron flux variations at low altitudes measured onboard CORONAS-I satellite, their connection with the particle flux variations in geosta-

tionary orbit, *Adv. Space Res.*, 2002, vol. 30, no. 10, pp. 2319–2323.

16. Kuznetsov, S.N. and Myagkova, I.N., Energetic trapped proton and electron flux variations at low altitudes measured onboard CORONAS-F satellite during 2001, August–December, their connection with the particle flux variations in geostationary orbit, *Geophys. Monogr. Ser.*, 2005, vol. 155, pp. 121–125.
17. Sergeev, V., Nishimura, Y., Kubyshkina, M., et al., Magnetospheric location of the equatorward prebreakup arc, *J. Geophys. Res.*, 2012, vol. 117, A01212. doi 10.1029/2011JA017154
18. Sergeev, V.A., Yakhnin, A.G., and Pellinen, R., Mutual location and magnetospheric sources of intrusion zones of energetic electrons, diffusive and discrete auroras in the substorm preparatory phase, *Geomagn. Aeron.*, 1983, vol. 23, no. 6, pp. 972–978.
19. Yahnin, A.G., Sergeev, V.A., Gvozdevsky, B.B., and Vennerstrom, S., Magnetospheric source region of discrete auroras inferred from their relationship with isotropy boundaries of energetic particles, *Ann. Geophys.*, 1997, vol. 15, pp. 943–958.
20. Riazantseva, M., Myagkova, I.N., Karavaev, M.V., et al., Enhanced energetic electron fluxes at the region of the auroral oval during quiet geomagnetic conditions November 2009, *Adv. Space Res.*, 2012, vol. 50, no. 5, pp. 623–631.

Translated by O. Pismenov